

Exceptional and regular spectra of a generalized Rabi model

Michael Tomka¹, Omar El Araby², Mikhail Pletyukhov³, Vladimir Gritsev²

¹*Department of Physics, Boston University, 590 Commonwealth Ave., Boston, MA 02215, USA*

²*Institute for Theoretical Physics, University of Amsterdam, Science Park 904, Postbus 94485, 1098 XH Amsterdam, The Netherlands*

³*Institute for Theory of Statistical Physics and JARA – Fundamentals of Future Information Technology, RWTH Aachen, 52056 Aachen, Germany*

We study the spectrum of a generalized Rabi model in which co- and counter-rotating terms have different coupling strengths. It is also equivalent to the model of a two-dimensional electron gas in a magnetic field with Rashba and Dresselhaus spin-orbit couplings. Like in case of the Rabi model, the spectrum of our generalized Rabi model consists of the regular and the exceptional parts. The latter is represented by the energy levels which cross at certain parameter values which we determine explicitly. The wave functions of these exceptional states are given by finite order polynomials in the Bargmann representation. The roots of these polynomials satisfy a Bethe ansatz equation of the Gaudin type. At the exceptional points the model is therefore quasi-exactly solvable. An analytical approximation is derived for the regular part of the spectrum in the weak- and strong-coupling limits. In particular, in the strong-coupling limit the spectrum consists of two ladders of equidistant levels.

PACS numbers: 42.50.Pq, 03.65.Ge, 03.65.Fd, 32.80.-t

I. INTRODUCTION

The Rabi model [1] is a fundamental model of light-matter interaction. It describes a single-mode photonic field interacting with a single two-level emitter,

$$\hat{H}_R = \omega \hat{a}^\dagger \hat{a} + \omega_0 \hat{\sigma}_z + g (\hat{a} + \hat{a}^\dagger) (\hat{\sigma}_+ + \hat{\sigma}_-), \quad (1)$$

where the bosonic operators \hat{a}, \hat{a}^\dagger describe the photons, and $\hat{\sigma}_\mu$, $\mu = z, \pm$, are the Pauli matrices describing a two-level emitter. When the coupling strength g/ω is small $\sim 10^{-2}$ and the near-resonance condition is satisfied, $\omega \sim 2\omega_0$, it is legitimate to make the rotating wave approximation (RWA) by neglecting the counter-rotating terms $\hat{a} \hat{\sigma}_-$ and $\hat{a}^\dagger \hat{\sigma}_+$. In this case, known as the Jaynes-Cummings (JC) model [2], the operator of the total number of excitations $\hat{N}_{\text{ex}} = \hat{a}^\dagger \hat{a} + \hat{\sigma}_+ \hat{\sigma}_-$ is a conserved quantity which ensures exact solvability of the JC model. On the other hand, in the Rabi model the only conserved quantity is the parity $\hat{\Pi} = \exp(i\pi \hat{N}_{\text{ex}})$. The question of exact solvability of the Rabi model has been debated for a long time, and the recent renewal of interest to the subject [3], [4] has been motivated by the rapid experimental progress in quantum optics. Several regimes of the Rabi model (1) are usually distinguished in the literature depending on the coupling strength or the detuning $\Delta = \omega - 2\omega_0$. In terms of the dimensionless parameter $\eta = g/\omega$ these are: (i) the weak-coupling regime, when the JC model is applicable, $\eta \sim 10^{-2}$; (ii) the strong-coupling regime, $10^{-2} < \eta < 0.1$; (iii) the ultra-strong coupling regime, $0.1 < \eta < 1$, and (iv) deep strong-coupling regime $\eta > 1$. For sufficiently large detuning so that $|\Delta| \gg 2\omega_0$, the RWA breaks down even for a relatively weak coupling. If couplings of the field and the emitter to dissipative baths (γ and Γ , respectively) are included, it is often assumed that the cooperativity factor $\xi = g^2/\gamma\Gamma$ is large enough to ensure almost

coherent short time evolution. It is worth noting that the standard weak-coupling master (Lindblad) equation approach to dissipative dynamics in the strong-coupling regime should be taken with caution [5]. Namely, the reduced density matrix equation should be expressed in terms of exact eigenstates of the isolated subsystem. This calls for detailed studies of the spectrum in the different limits (i)-(iv). Experimentally, the weak-coupling regime is achieved in cavity QED setups [6], while the regimes up to the ultra-strong coupling have been recently accessed using circuit QED systems [7], [8].

The analytical solution of the Rabi model in terms of transcendental functions has been found recently in Ref. [3]. On the other hand, several analytical approximations are also available. Thus, uniformly approximate results for energy levels valid in the whole range of parameters were found in [9]; also known are the approximation based on the polaron-like transformation, which is valid in the intermediate coupling (Bloch-Siegert) regime [10], the adiabatic approximation valid in the strong-coupling regime [11], and the deep strong-coupling approximation [12].

A complementary information on the spectrum of the Rabi model is provided by the *quasi-exact solutions* (QES). Indeed, it was observed [13], [14], [15], [16], [17], [18], [19] that the spectrum of the Rabi model has both regular and exceptional pieces. The exceptional parts of the spectrum are those whose wave functions are finite-order polynomials in the Bargmann representation. The energies of the exceptional solution are integer-valued $E = n\omega - g^2/\omega$, where for every n there is a special (polynomial) condition on the model parameters for which this solution is valid. It was proven in [15] that two neighboring levels cross on parallel straight lines $E = n\omega - g^2/\omega$ in parameter space. Moreover, for

each n the number of such crossings is precisely n , and there are no other crossings away from these lines. The connection of exceptional solutions with the concept of quasi-exact solvability (see [20] for an extensive review and references) has been discussed in [18]. We also note that in the quasi-classical regime the model exhibits chaotic behavior, and the exceptional solutions correspond to the isolated set of periodic orbits [21].

In this paper we study a generalized Rabi model

$$\hat{H}_{\text{gR}} = \omega \hat{a}^\dagger \hat{a} + \omega_0 \hat{\sigma}_z + g_1 (\hat{a}^\dagger \hat{\sigma}_- + \hat{a} \hat{\sigma}_+) + g_2 (\hat{a}^\dagger \hat{\sigma}_+ + \hat{a} \hat{\sigma}_-), \quad (2)$$

which interpolates between the JC model ($g_2 = 0$) and the original Rabi model ($g_1 = g_2$). There are several motivations to consider this model. First, as observed in [22] it can be mapped onto the model describing a two-dimensional electron gas with Rashba ($\alpha_R \sim g_1$) and Dresselhaus ($\alpha_D \sim g_2$) spin-orbit couplings subject to a perpendicular magnetic field (the Zeeman splitting thereby equals $2\omega_0$). The Rashba spin-orbit coupling can be tuned by an applied electric field while the Zeeman term is tuned by an applied magnetic field. This allows us to explore the whole parameter space of the model. Second, the model can directly emerge in quantum optics in the context of cavity QED [23] beyond the dipole approximation. For example in Ref. [24] a realization of the generalized Rabi model (2) based on resonant Raman transitions in an atom interacting with a high finesse optical cavity mode is proposed.

Here we describe the exceptional solutions of the model (2). As in the Rabi model we find exceptional points corresponding to doubly-degenerate level crossings in parameter space $(\omega, \omega_0, g_1, g_2)$. These degeneracies (intersection points) form curves whose equations can be determined from a set of algebraic conditions. The level intersections occur only at integer values of the energy $\frac{E}{\omega} + \frac{g_1^2 + g_2^2}{2\omega^2}$, and no intersections are observed elsewhere. We discuss several interesting links between the structure of the exceptional solutions and quasi-exact solvability, and the Gaudin-type Bethe ansatz solvable models. Namely, the conditions that the parameters of the generalized Rabi model need to satisfy such that the energy levels are doubly-degenerate, are given in terms of Bethe ansatz equations that have the same form as those of a reduced Richardson model from superconductivity theory. The pairing interaction strength of the conduction electrons corresponds then to $\omega^2/(2g_1g_2)$ from our generalized Rabi model.

Moreover, we analyze the weak- and strong-coupling limits of the regular spectrum. In particular, we show that in the strong-coupling limit the spectrum consists of two ladders of quasi-degenerate equidistant levels for a small splitting of the two-level system, $\omega_0 \ll \omega$. Whereas for $\omega_0 \gg \omega$ the spectrum is similar to the one of the JC model. We supplement our analytical study by comprehensive numerical calculations.

The paper is organized as follows. In Sec. II we present the procedure of determining the exceptional part of the

spectrum of the generalized Rabi model (2). It is shown that, as in the case of the Rabi model, the exceptional part corresponds to doubly-degenerate level crossings for which the associated eigenfunctions in Bargmann space are polynomials of finite order. Further, we establish explicitly the conditions on the system parameters at which these level crossings occur. We consider also the limits where the exceptional solutions can be determined analytically. In Sec. III we discuss two limiting cases of the regular part of the spectrum, namely a weak coupling limit of either small g_1 or small g_2 and a strong coupling limit for large values of both g_1 and g_2 . Section IV contains the conclusions of the present work.

II. EXCEPTIONAL SOLUTIONS FOR THE GENERALIZED RABI HAMILTONIAN

A. Hamiltonian in Bargmann representation

To determine the exceptional solutions of the generalized Rabi model (2) we use the Bargmann representation for the bosonic creation and annihilation operators in the space of analytic functions in a complex variable z ,

$$\hat{a} \rightarrow \frac{d}{dz}, \quad \hat{a}^\dagger \rightarrow z. \quad (3)$$

Then, after applying the transformation $\hat{\mathcal{H}} = \hat{P}\hat{H}_{\text{gR}}\hat{P}^{-1}$, with

$$\hat{P} = \begin{pmatrix} -\frac{1}{2} \frac{\sqrt{g_2}}{\sqrt{g_1}} & \frac{1}{2} \\ \frac{1}{2} \frac{\sqrt{g_2}}{\sqrt{g_1}} & \frac{1}{2} \end{pmatrix}, \quad \hat{P}^{-1} = \begin{pmatrix} -\frac{\sqrt{g_1}}{\sqrt{g_2}} & \frac{\sqrt{g_1}}{\sqrt{g_2}} \\ 1 & 1 \end{pmatrix}, \quad (4)$$

the stationary Schrödinger equation $\hat{\mathcal{H}}\psi = E\psi$ for the two component wave function,

$$\psi(z) = \begin{pmatrix} \psi_1(z) \\ \psi_2(z) \end{pmatrix}, \quad (5)$$

becomes a system of two first-order linear differential equations for the functions $\psi_1(z)$ and $\psi_2(z)$

$$(z - \nu) \frac{d\psi_1}{dz} - \left(\frac{\lambda_+}{\nu} z + e \right) \psi_1 + \left(\frac{\lambda_-}{\nu} z - \delta \right) \psi_2 = 0, \quad (6)$$

$$(z + \nu) \frac{d\psi_2}{dz} + \left(\frac{\lambda_+}{\nu} z - e \right) \psi_2 - \left(\frac{\lambda_-}{\nu} z + \delta \right) \psi_1 = 0, \quad (7)$$

where we introduced the dimensionless quantities

$$\begin{aligned} \delta &\equiv \frac{\omega_0}{\omega}, & \lambda_{\pm} &\equiv \frac{\frac{1}{2}(g_1^2 \pm g_2^2)}{\omega^2}, & \nu &\equiv \frac{\sqrt{g_1 g_2}}{\omega}, \\ e &\equiv \frac{E}{\omega}, & \epsilon &\equiv e + \lambda_+. \end{aligned} \quad (8)$$

In analogy to the Rabi model [15] we study the analytical properties of the solutions $\psi_1(z)$ and $\psi_2(z)$ around

the two singular points $z = \pm\nu$. To this end we expand the solutions as power series about one of the singular points $z = \nu$:

$$\psi_i(z) = (z - \nu)^s \sum_{n=0}^{\infty} c_n^{(i)} (z - \nu)^n, \quad i = 1, 2. \quad (9)$$

Inserting this expansion into Eqs. (6) and (7) yields the so-called indicial equation

$$s(\lambda_+ + e - s) = 0, \quad (10)$$

for the possible values of s . We note that the same condition is found for the singularity $z = -\nu$. The first solution $s = 0$ of Eq. (10) shows that we can always find an analytic solution $\psi(z) = (\psi_1(z), \psi_2(z))^T$ in a neighborhood of the singularities $z = \pm\nu$. The second solution $s = \lambda_+ + e$ implies that another linearly independent analytic solution $\tilde{\psi}(z)$ can occur and then the energy level is doubly degenerate. But this second solution is only analytic if the energy satisfies $e = n - \lambda_+$, where n is a non-negative integer, and in this case is given by $\tilde{\psi}(z) = (\psi_2(-z), \psi_1(-z))^T$. The exact condition on the other parameters for which these doubly degenerated exceptional solutions appear will be determined in the following. We will show that these solutions are polynomials of finite order.

Differentiating Eq. (6) one more time and eliminating $\psi_2(z)$ from Eq. (7) and $\psi_2'(z)$ from Eq. (6), we get a second-order differential equation for $\psi_1(z)$. After some transformations (see Appendix A) these equations can be written as

$$\left[\frac{d^2}{dz^2} + \left(\sum_{s=1}^3 \frac{\nu_s}{z - \rho_s} + \nu_0 \right) \frac{d}{dz} + \frac{D_2(z)}{\prod_{s=1}^3 (z - \rho_s)} \right] \chi(z) = 0, \quad (11)$$

where $D_2(z) = \sum_{s=0}^2 d_s z^s$ is a polynomial of degree 2 with coefficients given by

$$d_0 = \kappa (\delta^2 - \epsilon^2 + 2\epsilon\lambda_+ - \lambda_+^2 + \lambda_+ + \nu^2 + \nu^4) + \nu (\epsilon - \lambda_+ - \nu^2), \quad (12)$$

$$d_1 = e(e+1) - \delta^2 + \delta \frac{\lambda_+}{\lambda_-} + \nu\kappa - \nu^2 - 2\nu\epsilon\kappa - \nu^4, \quad (13)$$

$$d_2 = 2\nu\epsilon, \quad (14)$$

and $\chi(z) = \exp(\nu z)\psi_1(z)$. The other constants in Eq. (11) are

$$\rho_1 = \nu, \quad \rho_2 = -\nu, \quad \rho_3 = \kappa, \quad (15)$$

$$\nu_1 = -\epsilon + 1, \quad \nu_2 = -\epsilon, \quad \nu_3 = -1, \quad \nu_0 = -2\nu, \quad (16)$$

where we set

$$\kappa \equiv \frac{\delta\nu}{\lambda_-} = \frac{2\omega_0\sqrt{g_1g_2}}{g_1^2 - g_2^2}. \quad (17)$$

Note that the differential equation (11) is more general than the one corresponding to the usual Rabi model with $g_1 = g_2 = g$, yet it also has a polynomial solution

$$\chi(z) = \prod_{i=1}^n (z - z_i) \quad (18)$$

of degree n , if the coefficients d_j satisfy certain relations. These were explicitly found [25] using the functional Bethe ansatz method [26]. This method simply consists in inserting $\chi(z)$ into Eq. (11) and then dividing by $\chi(z)$. The resulting equation gives then rise to the conditions that the coefficients d_j need to satisfy such that $\chi(z)$ is a valid solution of Eq. (11). In our case these conditions read

$$d_2 = 2\nu n, \quad (19)$$

$$d_1 = 2\nu Z_1 - n \left[(n-1) + \sum_{s=1}^3 \nu_s + 2\nu \sum_{s=1}^3 \rho_s \right], \quad (20)$$

$$d_0 = 2\nu Z_2 - \left[2(n-1) + \sum_{s=1}^3 \nu_s + 2\nu \sum_{s=1}^3 \rho_s \right] Z_1 + n(n-1) \sum_{s=1}^3 \rho_s + n \left[2\nu \sum_{s<p}^3 \rho_s \rho_p + \sum_{s \neq p \neq q}^3 \nu_s (\rho_p + \rho_q) \right], \quad (21)$$

where $Z_k = \sum_{i=1}^n z_i^k$ and z_i are the roots of the Bethe ansatz equations

$$\sum_{j \neq i}^n \frac{2}{z_i - z_j} + \sum_{s=1}^3 \frac{\nu_s}{z_i - \rho_s} + \nu_0 = 0, \quad (22)$$

explicitly

$$\sum_{j \neq i}^n \frac{2}{z_j - z_i} + \frac{\epsilon - 1}{z_i - \nu} + \frac{\epsilon}{z_i + \nu} + \frac{1}{z_i - \kappa} + 2\nu = 0, \quad (23)$$

with $i = 1, 2, \dots, n$. Eqs. (14) and (19) yield the allowed

energy spectrum,

$$\epsilon = n, \quad \text{or} \quad E = \omega(n - \lambda_+). \quad (24)$$

Substituting this into the second and the third conditions, Eqs. (20), (21), gives

$$2\nu Z_1 = \lambda_+^2 - \left(2n + 1 - \frac{\kappa}{\nu}\right) \lambda_+ - (\delta^2 + \nu(\nu - \kappa) + \nu^4), \quad (25)$$

$$2\nu^2 Z_2 = -\lambda_+^2 + \left(2n + 1 - \frac{\kappa}{\nu} + \kappa^2 - \nu^2\right) \lambda_+ + (\delta^2 + \nu(\nu - \kappa) + \kappa^2 \nu^2 + 2n\nu^2(\nu^2 + 1)), \quad (26)$$

where $\lambda_+ = \sqrt{\delta^2 \frac{\nu^2}{\kappa^2} + \nu^4}$, which comes from the identity $\lambda_+^2 - \lambda_-^2 = \nu^4$. A derivation of those formulas can be found in Appendix B.

B. Analysis of the spectrum: exceptional case

The procedure for determining the locations of the exceptional solutions in the parameter space is now the following: by fixing the number of nodes n of the eigenfunctions $\chi(z)$ and three out of the four parameters $(\omega, \omega_0, g_1, g_2)$, we solve the Bethe ansatz equations (23) according to the method proposed in [27] under the conditions (24), (25) and (26). This yields a polynomial equation for the remaining parameter. The solutions of this polynomial equation provides us the values of the remaining parameter for which the eigenfunctions $\chi(z)$ are given by a polynomial of order n in the Bargmann representation. A detailed explanation of this procedure is presented in Appendix C.

The condition for an existence of polynomial solutions implies that the two solutions $\psi(z)$ and $\tilde{\psi}(z)$ mentioned after Eq. (10) are degenerate with the eigenenergies given by (24). Away from these exceptional points these degeneracies are lifted.

The exceptional solutions correspond therefore to the doubly-degenerate energy level crossings in parameter space. We note that the polynomial solutions obtained for the exceptional part of the spectrum can be related to the generalized Heine-Stieltjes polynomials [28].

It is interesting to realize that the Bethe ansatz equations (23) have the same form as those for the reduced BCS (Richardson) model having three degenerate levels of energies $\rho_{1,2,3}$ with degeneracies $\nu_{1,2,3}$ respectively. This corresponding physical model is integrable and can be derived from the generalized Gaudin models (see, e.g., [29] for review). Interestingly, the energy of that reduced BCS model is proportional to Z_1 up to an additive constant. We would like to point out that there is no known mapping between the two models. We therefore understand this connection rather as a generic mathematical structure behind Gaudin-type models and polynomial solutions of the differential equations. This common structure is nothing else than the electrostatic anal-

ogy which has been discussed extensively in the literature, see e.g. [30] for the case of differential equations and [29] for Gaudin-type models.

In general, the Bethe equations can be analyzed using the mapping to the Riccati hierarchy [27]. The case of $\kappa^2 = \nu^2$ requires special attention. In this case $\delta = \pm\lambda_-$ the Bethe ansatz equations are those of the degenerate two-step model [31]. Namely, when $\delta = -\lambda_-$ (so that $\kappa = -\nu$) the three roots $\rho_{1,2,3}$ degenerate into two (namely to $\pm\nu$) and moreover, the polynomial $D_2(z)$ is factorized as $D_2(z) = (z + \nu)(2\nu\epsilon z + d_0/\nu)$ which simplifies the differential and the Bethe ansatz equations. The corresponding conditions are given in Ref. [25], Eqs. A.12-A.14 for $\sigma = 0$.

One of the central results of this paper is that the conditions determining the locations of the exceptional solutions in parameter space are given through the Bethe ansatz equations (23), which are the same as those of the reduced BCS model. Those exceptional solutions occur only at $\epsilon = n$, exactly where the energy levels cross. The corresponding eigenstates are therefore doubly degenerate and have no definite parity. They can be expressed as a product of a polynomial of finite order and an exponential function in the Bargmann representation $\psi(z) \propto e^{-\nu z} \prod_{i=1}^n (z - z_i)$, where the zeros z_i are given by the roots of the Bethe ansatz equation (23).

Using numerical diagonalization we plot the spectrum of the generalized Rabi model in Fig. 9 for a range of coupling parameters. These calculations fully confirm our expectations about the number and positions of exceptional points, the energy level crossings. Below (see Sec. II B 1) we analyze several examples of the solution in more detail.

The number of exceptional solutions for a given integer energy $\epsilon = n$, is determined by the number of real solutions of the polynomial equation obtained by solving the Bethe ansatz equations (23), $p_n(\kappa, \nu, \delta) = 0$ (see Appendix C). In Fig. 1 we plot the number of exceptional solutions, N_{cr} , for the first eight integer energies $n = 0, 1, \dots, 7$ as a function of ω_0 and for fixed photon frequency $\omega = 1$ and coupling $g_2 = 0.01$. We find that N_{cr} is always between $n + 1$ and $2n + 1$. In Sec. III A 2 we use a degenerate perturbation theory to show that N_{cr} depends on the detuning $|\omega - 2\omega_0|$ and that $n + 1 \leq N_{cr} \leq 2n + 1$.

1. Examples

Let us first consider $\epsilon = n = 0$. In this case the Bethe ansatz equations are degenerate, $Z_1 = Z_2 = 0$ and the two conditions Eq. (25) and Eq. (26) are satisfied simultaneously as soon as $\kappa = \nu$, that is when $\lambda_- = \delta$. In Fig. 2 we plot the two lowest eigenenergies ϵ of $\hat{H}_{\text{gR}}/\omega + (g_1^2 + g_2^2)/2\omega^2$ as a function of g_1 and g_2 . They cross precisely in the plane $\epsilon = 0$ and on the curves $\lambda_- = \delta$ (bold red line). In terms of the original parameters these curves are given by

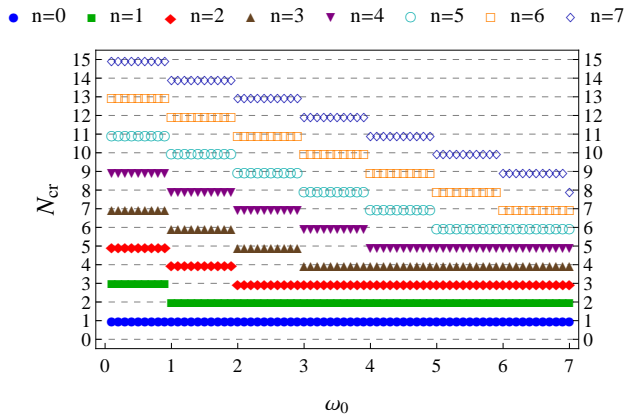


FIG. 1: Number of energy level crossings, N_{cr} , for a given integer energy n as a function of ω_0 for $\omega = 1$ and $g_2 = 0.01$.

$g_1^2 - g_2^2 = 2\omega\omega_0$. The corresponding eigenstates are $|\psi_0\rangle = \frac{1}{\sqrt{2}}(|\nu\rangle|+\rangle \pm |-\nu\rangle|-\rangle)$, so-called cat states [32], where $|\nu\rangle = \exp(-\nu^2/2)\exp(\nu\hat{a}^\dagger)|0\rangle$ is a coherent state with $\nu = \sqrt{g_1g_2}/\omega$ and $|\pm\rangle$ are the eigenstates of $\hat{\sigma}_z$.

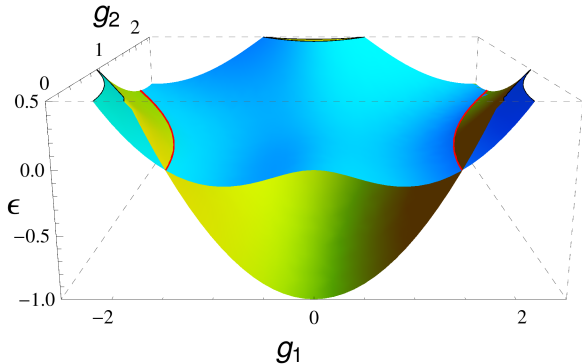


FIG. 2: Plot of the lowest two energies of \hat{H}_{GR}/ω shifted by the constant $(g_1^2 + g_2^2)/(2\omega^2)$, as a function of g_1 and g_2 for $\omega = \omega_0 = 1$. The energies were calculated by numerical diagonalization. The bosonic Hilbert space $\{|n\rangle\}$ was truncated by $n_{max} = 200$. The yellow plane corresponds to the lowest energy level and the cyan plane to the energy of the first excited state. They cross exactly in the plane of $\epsilon = 0$. The lines on which these energy levels cross is given by $g_1^2 - g_2^2 = 2\omega\omega_0$ (red line) as predicted by the quasi-exact solutions.

For $\epsilon = n = 1$ the Bethe ansatz equations (23) can be solved analytically

$$z_{1,\pm} = \frac{\kappa\nu - \nu^2 - 1 \pm \sqrt{\nu^2(\kappa + \nu)^2 + 1}}{2\nu}. \quad (27)$$

The locations of the exceptional solutions in parameter space are obtained as follows. By inserting this expression for the Bethe root $z_{1,\pm}$ into the two conditions Eq. (25) and Eq. (26), we get a polynomial equation for the parameters κ , ν and δ , which we denote by

$p_1(\kappa, \nu, \delta) = 0$. The real zeros of this equation determine the positions of the exceptional solutions in parameter space. The values of the original parameters are obtained by inverting the expressions for κ , ν and δ :

$$g_1 = \omega \sqrt{\frac{\nu}{\kappa}} \sqrt{\delta + \sqrt{\delta^2 + \kappa^2\nu^2}}, \quad (28)$$

$$g_2 = \omega \sqrt{\frac{\kappa}{\nu}} \frac{\nu^2}{\sqrt{\delta + \sqrt{\delta^2 + \kappa^2\nu^2}}}, \quad (29)$$

$$\omega_0 = \omega\delta. \quad (30)$$

We note that for a given energy level crossing only one of the two possible Bethe roots $z_{1,\pm}$ yields a real solution to the equation $p_1(\kappa, \nu, \delta) = 0$, which we call z_1^* . The corresponding eigenstates are as expected doubly degenerate $|\psi_1\rangle = \frac{1}{\sqrt{2}}((\hat{a}^\dagger - z_1^*)|\nu\rangle|+\rangle \pm (\hat{a}^\dagger + z_1^*)|-\nu\rangle|-\rangle)$.

For $\epsilon = n > 1$ we have to solve the Bethe equations (23) numerically by the procedure described in Appendix C to obtain the positions of the energy level crossings in parameter space. In Fig. 3 we computed the values of Z_1 and Z_2 for $n = 5$ and $\kappa = 0.1$ as a function of ν . We find exactly 10 different solutions for Z_1 and Z_2 . Inserting each corresponding pair of Z_1 and Z_2 into Eq. (25) and Eq. (26) yields a polynomial equation for δ . The real zeros of this equation gives the values of δ at which the energy levels cross on the line $\epsilon = 5$.

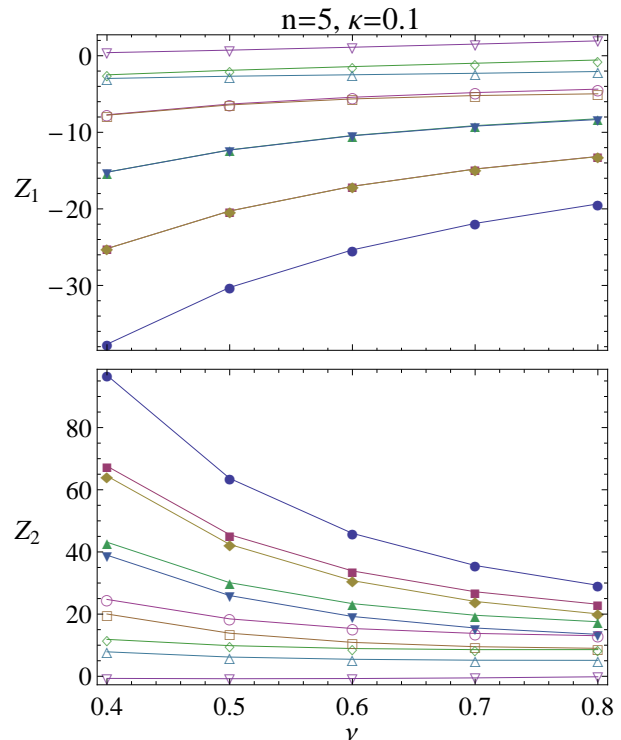


FIG. 3: $Z_1 = \sum_{i=1}^n z_i$ and $Z_2 = \sum_{i=1}^n z_i^2$ as functions of ν for $n = 5$ and $\kappa = 0.1$. Note that some lines are nearly degenerate.

2. Limiting cases

For some limits the form of the curves corresponding to exceptional solutions can be determined analytically. Here we use results known for the reduced BCS (Richardson) model. First, we rescale the roots $z_j = \nu x_j$ and rewrite (23) as

$$\sum_{j \neq i}^n \frac{2}{x_j - x_i} + \frac{\epsilon - 1}{x_i - 1} + \frac{\epsilon}{x_i + 1} + \frac{1}{x_i - \frac{\kappa}{\nu}} + 2\nu^2 = 0, \quad (31)$$

known as the Richardson equations in the BCS context $g_{\text{BCS}} = (2\nu^2)^{-1}$. The BCS pair energy levels are given by $E_{1,2} = \pm 1$ and the limit $\nu \rightarrow 0$ corresponds to the strong-coupling limit in the sense of the BCS model. In this case the structure of the roots $\{x_j\}$ for the Richardson ground state solution (for which all the Bethe roots diverge) reads [33]

$$x_j = \frac{1}{2\nu^2} y_j + \frac{1}{2n} \left(\frac{\kappa}{\nu} - 1 \right) + O(\nu^2), \quad (32)$$

where y_j are the roots of the associated Laguerre polynomials $L_n^{(-1-2n)}(y)$. Representing $L_n^{(\alpha)}(y) = ((-1)^n/n!) \prod_{j=1}^n (y - y_j)$, one can derive the sum of the roots

$$\begin{aligned} \sum_{j=1}^n y_j &= -n\nu \frac{d^{(n-1)}}{dy^{(n-1)}} L_n^{(\alpha)}(y) \Big|_{y=0} \\ &= nL_1^{(\alpha+n-1)}(0) = n(n+\alpha), \end{aligned} \quad (33)$$

as well as

$$\sum_{j < k} y_j y_k = n(n-1)(n+\alpha)(n+\alpha-1)/2, \quad (34)$$

$$\sum_{j=1}^n y_j^2 = n(n+\alpha)(2n+\alpha-1). \quad (35)$$

It follows then

$$Z_1 = \frac{-n(n+1)}{2\nu} + \frac{\nu}{2} \left(\frac{\kappa}{\nu} - 1 \right), \quad (36)$$

$$Z_2 = \frac{n(n+1)}{2\nu^2} - \frac{n+1}{2} \left(\frac{\kappa}{\nu} - 1 \right) + \frac{\nu^2}{4n} \left(\frac{\kappa}{\nu} - 1 \right)^2. \quad (37)$$

For the other solutions one must consider the various combinations of diverging and non diverging roots. More details are given in [34]. Interestingly, in the opposite limit of weak-coupling $g_{\text{BCS}} \rightarrow 0$ the roots can be expressed in terms of the Laguerre polynomials (see the Refs. [34] and [27]) and the analytical expressions for $Z_{1,2}$ can also be found.

In Fig. 4 we illustrate the analytically calculated limit $\nu \rightarrow 0$ of Z_1 and Z_2 (red line) compared with some numerical values (blue dots) for $n = 5$ and $\kappa = 0.1$. This is consistent with the ground state solutions of the Richardson equations.

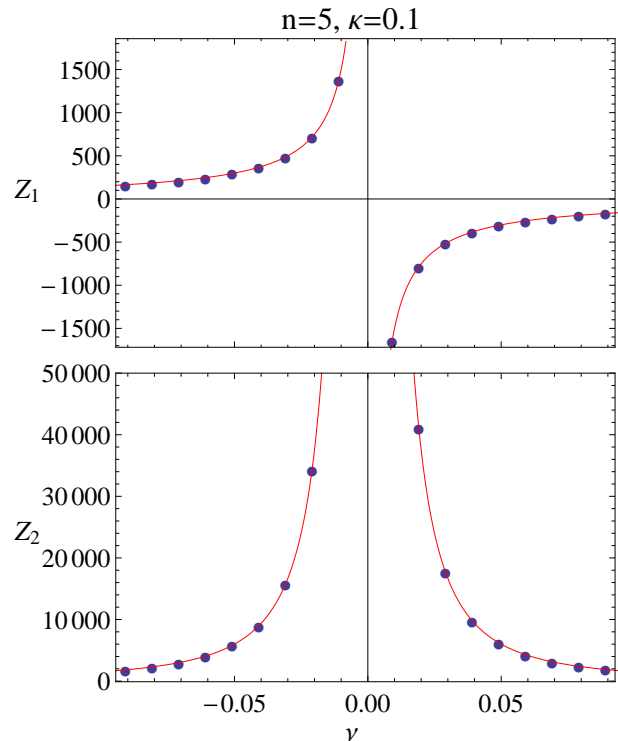


FIG. 4: Comparison of the analytical limit (red line) and numerically calculated (blue dots) values of Z_1 and Z_2 for $n = 5$, $\kappa = 0.1$ and $\nu \rightarrow 0$.

III. REGULAR SPECTRUM OF THE GENERALIZED RABI HAMILTONIAN: LIMITS

Here we consider the two limiting cases for the regular part of the spectrum: (i) the limit of either small g_1 or small g_2 , and (ii) the limit of both large g_1 and g_2 . We show that in the latter case the spectrum is a superposition of two quasi-degenerate harmonic ladders.

A. Limit of small g_1 or small g_2

Let us focus first on the case of small g_2 , $g_2 \ll g_1$. In this limit we consider the counter-rotating part $\hat{H}_{g_2} = g_2(\hat{a}^\dagger \hat{\sigma}_+ + \hat{a} \hat{\sigma}_-)$ as a perturbation to the Jaynes-Cummings model $\hat{H}_0 = \omega \hat{a}^\dagger \hat{a} + \omega_0 \hat{\sigma}_z + g_1(\hat{a}^\dagger \hat{\sigma}_- + \hat{a} \hat{\sigma}_+)$. For the unperturbed part \hat{H}_0 we know the eigenenergies [2]

$$E_{n,k}^{(0)} = \omega \left(n + \frac{1}{2} \right) + (-1)^k \Omega_n, \quad (38)$$

$$\Omega_n = \sqrt{\left(\omega_0 - \frac{\omega}{2} \right)^2 + g_1^2 (n+1)}, \quad (39)$$

with $k = 0, 1$ and the eigenstates

$$|n, 0\rangle = \cos \frac{\alpha_n}{2} |n, +\rangle + \sin \frac{\alpha_n}{2} |n+1, -\rangle, \quad (40)$$

$$|n, 1\rangle = -\sin \frac{\alpha_n}{2} |n, +\rangle + \cos \frac{\alpha_n}{2} |n+1, -\rangle, \quad (41)$$

where

$$\cos \alpha_n = \frac{\omega_0 - \frac{\omega}{2}}{\Omega_n}, \quad \sin \alpha_n = \frac{g_1 \sqrt{n+1}}{\Omega_n}. \quad (42)$$

The bare basis states are defined by $|n, \pm\rangle = |n\rangle_{\text{field}} \otimes |\pm\rangle_{\text{atom}}$, the tensor product of the Fock states $|n\rangle_{\text{field}}$ and the eigenstates of $\hat{\sigma}_z$, $\hat{\sigma}_z |\pm\rangle_{\text{atom}} = \pm |\pm\rangle_{\text{atom}}$. The eigenstates $|n, k\rangle$ are simultaneously the eigenstates of the excitation number operator, $\hat{N}_{\text{ex}} |n, k\rangle = (n+1) |n, k\rangle$.

The second order correction to $E_{n,k}^{(0)}$ due to \hat{H}_{g_2} reads

$$\begin{aligned} \frac{1}{g_2^2} E_{n,0}^{(2)} = & -\frac{n+2}{4\Omega_n} \frac{\Omega_n - \omega_0 + \frac{\omega}{2} - (n+1) \frac{g_1^2}{2\omega}}{\omega - \Omega_n - \frac{g_1^2}{2\omega}} \\ & + \frac{n}{4\Omega_n} \frac{\Omega_n + \omega_0 - \frac{\omega}{2} + (n+1) \frac{g_1^2}{2\omega}}{\omega + \Omega_n + \frac{g_1^2}{2\omega}}, \end{aligned} \quad (43)$$

$$\begin{aligned} \frac{1}{g_2^2} E_{n,1}^{(2)} = & -\frac{n+2}{4\Omega_n} \frac{\Omega_n + \omega_0 - \frac{\omega}{2} + (n+1) \frac{g_1^2}{2\omega}}{\omega + \Omega_n - \frac{g_1^2}{2\omega}} \\ & + \frac{n}{4\Omega_n} \frac{\Omega_n - \omega_0 + \frac{\omega}{2} - (n+1) \frac{g_1^2}{2\omega}}{\omega - \Omega_n + \frac{g_1^2}{2\omega}}. \end{aligned} \quad (44)$$

We note that the denominators in (43) and (44) can diverge. In the following we will show that these singularities occur at the energy levels crossings of \hat{H}_0 for which the eigenenergies $E_{n,k}^{(0)} + \frac{g_1^2 + g_2^2}{2\omega}$ are half-integer-valued, and that those singularities correspond to the avoided level crossings in the spectrum of $\hat{H}_{\text{gR}}/\omega + \lambda_+$ at *half-integer* energies.

Let us first consider the regime $\omega\sqrt{2} > g_1$. In this regime there are two singularities: 1a) $\omega = \Omega_n + \frac{g_1^2}{2\omega}$, which corresponds to the degeneracy of the levels

$$E_{n,0}^{(0)} = E_{n+2,1}^{(0)} = \omega(n + \frac{3}{2}) - \frac{g_1^2}{2\omega}, \quad (45)$$

or $-2\omega + \Omega_n + \Omega_{n+2} = 0$. The solution of this equation is given by

$$\frac{g_1^2}{2\omega} = \omega \left[n+2 - \sqrt{(n+1)(n+3) + \left(\frac{1}{2} - \frac{\omega_0}{\omega}\right)^2} \right], \quad (46)$$

for $n = 0, 1, 2, \dots$

2a) $\omega = \Omega_n - \frac{g_1^2}{2\omega}$, which corresponds to the degeneracy of the levels

$$E_{n,1}^{(0)} = E_{n-2,0}^{(0)} = \omega(n - \frac{1}{2}) - \frac{g_1^2}{2\omega}, \quad (47)$$

or $2\omega - \Omega_n - \Omega_{n-2} = 0$. The solution of this equation is given by

$$\frac{g_1^2}{2\omega} = \omega \left[n - \sqrt{(n-1)(n+1) + \left(\frac{1}{2} - \frac{\omega_0}{\omega}\right)^2} \right], \quad (48)$$

for $n = 2, 3, 4, \dots$

Second, we consider the regime $\omega\sqrt{2} < g_1$. In this regime there are also two singularities: 1b) $\omega = -\Omega_n + \frac{g_1^2}{2\omega}$, which corresponds to the degeneracy of the levels

$$E_{n,1}^{(0)} = E_{n+2,1}^{(0)} = \omega(n + \frac{3}{2}) - \frac{g_1^2}{2\omega}, \quad (49)$$

or $-2\omega - \Omega_n + \Omega_{n+2} = 0$. The solution of this equation is given by

$$\frac{g_1^2}{2\omega} = \omega \left[n+2 + \sqrt{(n+1)(n+3) + \left(\frac{1}{2} - \frac{\omega_0}{\omega}\right)^2} \right], \quad (50)$$

for $n = 0, 1, 2, \dots$

2b) $\omega = \Omega_n - \frac{g_1^2}{2\omega}$, which corresponds to the degeneracy of the levels

$$E_{n,1}^{(0)} = E_{n-2,1}^{(0)} = \omega(n - \frac{1}{2}) - \frac{g_1^2}{2\omega}, \quad (51)$$

or $2\omega - \Omega_n + \Omega_{n-2} = 0$. The solution of this equation is given by

$$\frac{g_1^2}{2\omega} = \omega \left[n + \sqrt{(n-1)(n+1) + \left(\frac{1}{2} - \frac{\omega_0}{\omega}\right)^2} \right], \quad (52)$$

for $n = 2, 3, 4, \dots$

0) In addition, we consider the corrections to the level $E_{-1,1}^{(0)}$ with the eigenstate $|-1, 1\rangle = |0, -\rangle$. The second order correction due to \hat{H}_{g_2} reads

$$\frac{1}{g_2} E_{-1,1}^{(2)} = \frac{1}{4} \frac{1}{\omega_0 + \frac{\omega}{2} - \frac{g_1^2}{2\omega}}. \quad (53)$$

Here the singularity can happen for $\Omega_1 = \omega_0 + \frac{3}{2}\omega$, which corresponds to the degeneracy of the levels

$$E_{-1,1}^{(0)} = E_{1,1}^{(0)} = \frac{\omega}{2} - \frac{g_1^2}{2\omega} \quad (54)$$

The solution of this equation is given by

$$\frac{g_1^2}{2\omega} = \omega_0 + \frac{\omega}{2}. \quad (55)$$

1. Degenerate perturbation theory

At the degeneracy points 1a)-2b) and 0) of the unperturbed Hamiltonian \hat{H}_0 , we need to use a degenerate perturbation theory to calculate the avoided level crossings of \hat{H}_{gR} .

In the case of 1a) the gap equals to

$$\begin{aligned}\Delta_{n,0;n+2,1} &= 2 |\langle n, 0 | \hat{H}_{g_2} | n+2, 1 \rangle| \\ &= 2g_2 \sqrt{n+2} \sin \frac{\alpha_n}{2} \sin \frac{\alpha_{n+2}}{2}.\end{aligned}\quad (56)$$

The case 2a) is obtained by the shift $n \rightarrow n-2$. At the degeneracy of 1b) the gap equals to

$$\begin{aligned}\Delta_{n,1;n+2,1} &= 2 |\langle n, 1 | \hat{H}_{g_2} | n+2, 1 \rangle| \\ &= 2g_2 \sqrt{n+2} \cos \frac{\alpha_n}{2} \sin \frac{\alpha_{n+2}}{2},\end{aligned}\quad (57)$$

and the case 2b) is again obtained by simply shifting $n \rightarrow n-2$. For the crossing of $E_{-1,1}^{(0)}$ and $E_{1,1}^{(0)}$, i.e. the case 0), we have

$$\begin{aligned}\Delta_{-1,1;1,1} &= 2 |\langle -1, 1 | \hat{H}_{g_2} | 1, 1 \rangle| \\ &= 2g_2 \sin \frac{\alpha_1}{2}.\end{aligned}\quad (58)$$

At these degeneracy points a meaningful approximation for the eigenenergies of \hat{H}_{gR} is given by

$$\begin{aligned}E_{n,k}^{(\pm)} &= \\ \frac{E_{n,k}^{(0)} + E_{n+2,1}^{(0)} \pm \sqrt{(E_{n,k}^{(0)} - E_{n+2,1}^{(0)})^2 + \Delta_{n,k;n+2,1}^2}}{2},\end{aligned}\quad (59)$$

where $(n = -1, k = 1)$ corresponds to the case 0), $(n = 0, 1, \dots, k = 0)$ represents the case 1a) and $(n = 0, 1, \dots, k = 1)$ gives the case 1b).

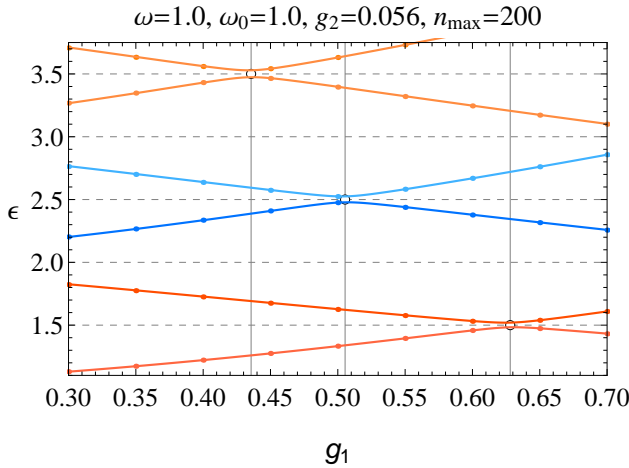


FIG. 5: The weak-coupling approximation given by Eq. (59) for the spectrum of the generalized Rabi model (full lines) compared with the numerical calculation of the spectrum (dots) for $g_2 = 0.056$ and $\omega = \omega_0 = 1$. Note that we added the constant $\lambda_+ = \frac{g_1^2 + g_2^2}{2\omega^2}$ to the Hamiltonian $\hat{H}_{\text{gR}}/\omega$ such that the level crossings occur at integer values and the avoided level crossings at half-integer values.

Other avoided level crossings can happen at $E_{n,k}^{(0)} = E_{n+2p,1}^{(0)}$ and $E_{-1,1}^{(0)} = E_{-1+2p,1}^{(0)}$, where $k = 0, 1$ and $p > 1$ is an integer. The corresponding gaps are $\Delta_{n,k;n+2p,1} \sim \mathcal{O}(g_2^p)$, since the corresponding eigenstates can only be connected in the perturbation theory by an application of \hat{H}_{g_2} at least p times.

Let us consider $p > 1$. Then

$$\Omega_{n+2p} \pm \Omega_n = 2p\omega \quad (60)$$

and

$$\Omega_{-1+2p} = \omega_0 + \omega(2p - \frac{1}{2}). \quad (61)$$

Eq. (60) has the solution for the upper sign ($k = 0$) at

$$\frac{g_1^2}{2\omega^2} = n + p + 1 - \sqrt{(n+1)(n+2p+1) + \left(\frac{1}{2} - \frac{\omega_0}{\omega}\right)^2}, \quad (62)$$

$$E_{n,0}^{(0)} = E_{n+2p,1}^{(0)} = \omega(n + p + \frac{1}{2}) - \frac{g_1^2}{2\omega}, \quad (63)$$

for $\omega\sqrt{2p} > g_1$. It is also important that the rhs of (62) is greater or equal to zero, which implies

$$p^2 \geq \left(\frac{1}{2} - \frac{\omega_0}{\omega}\right)^2. \quad (64)$$

The solutions for the lower sign ($k = 1$) takes place at

$$\frac{g_1^2}{2\omega^2} = n + p + 1 + \sqrt{(n+1)(n+2p+1) + \left(\frac{1}{2} - \frac{\omega_0}{\omega}\right)^2}, \quad (65)$$

$$E_{n,1}^{(0)} = E_{n+2p,1}^{(0)} = \omega(n + p + \frac{1}{2}) - \frac{g_1^2}{2\omega}, \quad (66)$$

for $\omega\sqrt{2p} < g_1$. Finally, Eq. (61) has the solution

$$\frac{g_1^2}{2\omega} = \omega_0 + \omega(p - \frac{1}{2}), \quad (67)$$

$$E_{-1,1}^{(0)} = E_{-1+2p,1}^{(0)} = \omega(p - \frac{1}{2}) - \frac{g_1^2}{2\omega}. \quad (68)$$

2. Number of crossings and avoided crossings

So we have seen that the avoided level crossings always happen at *half-integer* energies. By analogous considerations one can show that the crossings always happen at *integer* energies.

To find crossing points we need to solve the equations $E_{n,k}^{(0)} = E_{n+2p-1,1}^{(0)}$ and $E_{-1,1}^{(0)} = E_{-2+2p,1}^{(0)}$ for $p > 1$, which is equivalent to solve the equations

$$\Omega_{n+2p-1} \pm \Omega_n = (2p-1)\omega \quad (69)$$

$$\Omega_{-2+2p} = \omega_0 + \omega(2p - \frac{3}{2}). \quad (70)$$

Eq. (69) has the solutions for the upper sign ($k = 0$) at

$$\frac{g_1^2}{2\omega^2} = n + p + \frac{1}{2} - \sqrt{(n+1)(n+2p) + \left(\frac{1}{2} - \frac{\omega_0}{\omega}\right)^2}, \quad (71)$$

$$E_{n,0}^{(0)} = E_{n+2p-1,1}^{(0)} = \omega(n+p) - \frac{g_1^2}{2\omega}, \quad (72)$$

for $\omega\sqrt{2p-1} > g_1$. It is also important that the rhs of (71) is greater or equal to zero, which implies

$$\left(p - \frac{1}{2}\right)^2 \geq \left(\frac{1}{2} - \frac{\omega_0}{\omega}\right)^2 \quad \text{or} \quad p \geq \frac{1}{2} + \left|\frac{1}{2} - \frac{\omega_0}{\omega}\right|. \quad (73)$$

The solution for the lower sign ($k = 1$) takes place at

$$\frac{g_1^2}{2\omega^2} = n + p + \frac{1}{2} + \sqrt{(n+1)(n+2p) + \left(\frac{1}{2} - \frac{\omega_0}{\omega}\right)^2}, \quad (74)$$

$$E_{n,1}^{(0)} = E_{n+2p-1,1}^{(0)} = \omega(n+p) - \frac{g_1^2}{2\omega}, \quad (75)$$

for $\omega\sqrt{2p-1} < g_1$.

Eq. (70) has the solution

$$\frac{g_1^2}{2\omega} = \omega_0 + \omega(p-1), \quad (76)$$

$$E_{-1,1}^{(0)} = E_{-2+2p,1}^{(0)} = \omega(p-1) - \frac{g_1^2}{2\omega}. \quad (77)$$

To count the number of energy level crossings at a given integer N , we cast Eq. (72) to

$$E_{N-p,0}^{(0)} + \frac{g_1^2}{2\omega} = E_{N+p-1,1}^{(0)} + \frac{g_1^2}{2\omega} = \omega N, \quad (78)$$

with

$$\frac{1}{2} + \left|\frac{1}{2} - \frac{\omega_0}{\omega}\right| \leq p \leq N, \quad (79)$$

and Eq. (75) to

$$E_{N-p,1}^{(0)} + \frac{g_1^2}{2\omega} = E_{N+p-1,1}^{(0)} + \frac{g_1^2}{2\omega} = \omega N, \quad (80)$$

with

$$1 \leq p \leq N. \quad (81)$$

In addition, there is always one intersection of the levels

$$E_{-1,1}^{(0)} + \frac{g_1^2}{2\omega} = E_{2N,1}^{(0)} + \frac{g_1^2}{2\omega} = \omega N. \quad (82)$$

Thus, the number of crossings depends on the value of the detuning $|\omega - 2\omega_0|$. Analogously, we find the number of avoided level-crossings.

Finally, we would like to point out that the case of $g_1 \ll g_2$, can be reduced to the previous case by simply exchanging $g_1 \leftrightarrow g_2$ and flipping the sign of the level splitting $\omega_0 \rightarrow -\omega_0$ in all the formulas above, since $\hat{H}_{\text{gR}}(\omega, \omega_0, g_1, g_2) = \hat{T}^\dagger \hat{H}_{\text{gR}}(\omega, -\omega_0, g_2, g_1) \hat{T}$ where $\hat{T} = \exp(i\frac{\pi}{2}\hat{\sigma}_y) \exp(i\pi\hat{a}^\dagger\hat{a})$.

B. Strong-coupling limit

When the couplings g_1 and g_2 are both large we can identify two limits. One limit corresponds to small ω_0 the other to large ω_0 . In the former case the spectrum consists of two quasi-degenerate harmonic ladders, in the latter the spectrum is related to the solvable Jaynes-Cummings model.

1. Small ω_0 limit

In the strong-coupling limit, where both g_1 and g_2 are large and ω_0 is small, one can make use of the adiabatic approximation [11]. The idea behind this approximation for the Rabi model is to rotate the basis and to consider the term $\omega\hat{a}^\dagger\hat{a} + g\hat{\sigma}_x(\hat{a} + \hat{a}^\dagger)$ as a leading term which can be easily diagonalized, while the term $\omega_0\hat{\sigma}_z$ is treated as a perturbation. Generalizing this to our model we first rotate the spin basis $\hat{\sigma}_x \rightarrow \hat{\sigma}_y, \hat{\sigma}_y \rightarrow \hat{\sigma}_z, \hat{\sigma}_z \rightarrow \hat{\sigma}_x$ and write

$$\hat{H}_{\text{gR}} = \omega\hat{a}^\dagger\hat{a} + \beta(\hat{a} + \hat{a}^\dagger)\hat{\sigma}_z + i\lambda(\hat{a} - \hat{a}^\dagger)\hat{\sigma}_x + \omega_0\hat{\sigma}_y, \quad (83)$$

where $\beta = (g_1 + g_2)/2$ and $\lambda = (g_1 - g_2)/2$. In the adiabatic approximation the terms proportional to ω_0 and λ should be treated as a perturbation. Considering the basis $|\sigma\rangle \otimes |N_\sigma\rangle$, where $\sigma = \pm$ and $|N_\pm\rangle = \hat{D}(\mp\beta/\omega)|N\rangle$ with the Fock states $|N\rangle$ ($N = 0, 1, 2, \dots$) and the displacement operator $\hat{D}(\beta/\omega) = \exp((\beta/\omega)(\hat{a}^\dagger - \hat{a}))$, we obtain the eigenvalue equation for the leading term

$$\begin{aligned} \left[\left(\hat{a}^\dagger \pm \frac{\beta}{\omega}\right) \left(\hat{a} \pm \frac{\beta}{\omega}\right) \right] |\phi_\pm\rangle &\equiv \hat{D}\left(\mp\frac{\beta}{\omega}\right) \hat{a}^\dagger \hat{a} \hat{D}^\dagger\left(\mp\frac{\beta}{\omega}\right) |\phi_\pm\rangle \\ &= \left(\frac{E}{\omega} + \frac{\beta^2}{\omega^2}\right) |\phi_\pm\rangle. \end{aligned} \quad (84)$$

In this basis the Hamiltonian approximately has a block diagonal form with the N th block given by

$$\hat{H}_{\text{gR}}^{(N)} = \begin{pmatrix} E_N & h_{-,+} \\ h_{+,-} & E_N \end{pmatrix}, \quad (85)$$

where

$$h_{-,+} = -i\omega_0\langle N_-|N_+\rangle + i\lambda\langle N_-|(\hat{a} - \hat{a}^\dagger)|N_+\rangle, \quad (86)$$

$$h_{+,-} = i\omega_0\langle N_+|N_-\rangle + i\lambda\langle N_+|(\hat{a} - \hat{a}^\dagger)|N_-\rangle, \quad (87)$$

$$E_N = \omega(N - \beta^2/\omega^2), \quad (88)$$

provided the terms containing the overlaps $\langle N_\pm|M_\mp\rangle$ for $N \neq M$ are neglected. The overlap of the two displaced coherent states is

$$\langle M_-|N_+\rangle = e^{-2\beta^2/\omega^2} \left(\frac{2\beta}{\omega}\right)^{N-M} \sqrt{\frac{M!}{N!}} L_M^{N-M} \left(\frac{4\beta^2}{\omega^2}\right), \quad (89)$$

for $M < N$ and

$$\langle M_-|N_+\rangle = e^{-2\beta^2/\omega^2} \left(\frac{-2\beta}{\omega}\right)^{M-N} \sqrt{\frac{N!}{M!}} L_N^{M-N} \left(\frac{4\beta^2}{\omega^2}\right), \quad (90)$$

for $M \geq N$, while $\langle M_- | N_+ \rangle = (-1)^{N-M} \langle N_- | M_+ \rangle$ and $\langle M_+ | N_- \rangle = (-1)^{M-N} \langle M_- | N_+ \rangle$. The eigenenergies of the perturbed system are

$$E_N^\pm = E_N \pm |\omega_0 \langle N_- | N_+ \rangle - \lambda \langle N_- | (\hat{a} - \hat{a}^\dagger) | N_+ \rangle|. \quad (91)$$

To compute the necessary matrix elements we use the identities

$$\langle M_- | N_+ \rangle = \langle m | \hat{D}(-2\alpha) | n \rangle, \quad (92)$$

$$\begin{aligned} \langle M_- | \hat{a} | N_+ \rangle &= \langle m | \hat{D}(-\alpha) \hat{a} \hat{D}(-\alpha) | n \rangle \\ &= \langle m | \hat{D}(-2\alpha) \hat{D}(\alpha) \hat{a} \hat{D}(-\alpha) | n \rangle. \end{aligned} \quad (93)$$

It follows then

$$\begin{aligned} \langle M_- | \hat{a} | N_+ \rangle &= \langle m | \hat{D}(-2\alpha) (\hat{a} - \alpha) | n \rangle \\ &= \langle m | \hat{D}(-2\alpha) \left(\sqrt{N} |n-1\rangle - \alpha |n\rangle \right) \\ &= \sqrt{N} \langle M_- | (N-1)_+ \rangle - \alpha \langle M_- | N_+ \rangle \end{aligned} \quad (94)$$

and

$$\langle M_- | \hat{a}^\dagger | N_+ \rangle = \sqrt{N+1} \langle M_- | (N+1)_+ \rangle - \alpha \langle M_- | N_+ \rangle. \quad (95)$$

Thus we obtain the eigenenergies in the adiabatic approximation

$$E_N^\pm = E_N \pm e^{-2\beta^2/\omega^2} \left| \omega_0 L_N^0 \left(\frac{4\beta^2}{\omega^2} \right) + \lambda \frac{2\beta}{\omega} \left[L_{N-1}^1 \left(\frac{4\beta^2}{\omega^2} \right) + L_N^1 \left(\frac{4\beta^2}{\omega^2} \right) \right] \right|. \quad (96)$$

In the limiting case $g_1 = g_2 = g$ this equation agrees with the one obtained for the Rabi model in the limit of large g [11]. A similar approximation scheme for the Rabi model, using a ‘‘symmetrized generalized RWA’’ [36], also reproduces our result in the large g limit. We note that the second term introduces an exponentially small splitting when g_1 and g_2 are large and therefore the spectrum is a quasi-degenerate harmonic ladder. Fig. 6 illustrates the good agreement between Eq. (96) and the numerical results for $\omega_0 \ll \omega$ and $\lambda \ll 1$.

2. Large ω_0 limit

In this limit it is convenient to introduce the operators

$$\hat{A} = \frac{1}{g_-} (g_1 \hat{a} + g_2 \hat{a}^\dagger), \quad \hat{A}^\dagger = \frac{1}{g_-} (g_1 \hat{a}^\dagger + g_2 \hat{a}), \quad (97)$$

with $g_- \equiv \sqrt{g_1^2 - g_2^2}$, such that $[\hat{A}, \hat{A}^\dagger] = 1$ holds. We note that the operators \hat{A} and \hat{A}^\dagger are only well defined if $g_1 > g_2$. The operator $\hat{A}^\dagger \hat{A}$ is diagonal in the squeezed Fock states $|n, r\rangle = \hat{S}(r) |n\rangle$, where $\hat{S}(r) = \exp(\frac{1}{2} r (\hat{a}^\dagger)^2 - \frac{1}{2} r \hat{a}^2)$ and $\{|n\rangle\}$ are the eigenstates of $\hat{a}^\dagger \hat{a}$. So we have $\hat{A} = \hat{S} \hat{a} \hat{S}^\dagger = \cosh(r) \hat{a} + \sinh(r) \hat{a}^\dagger$ with $\tanh(r) = g_2/g_1$ and $\hat{A}^\dagger \hat{A} |n, r\rangle = n |n, r\rangle$, where $n = 0, 1, 2, \dots$

Using the operators \hat{A} and \hat{A}^\dagger we can rewrite the

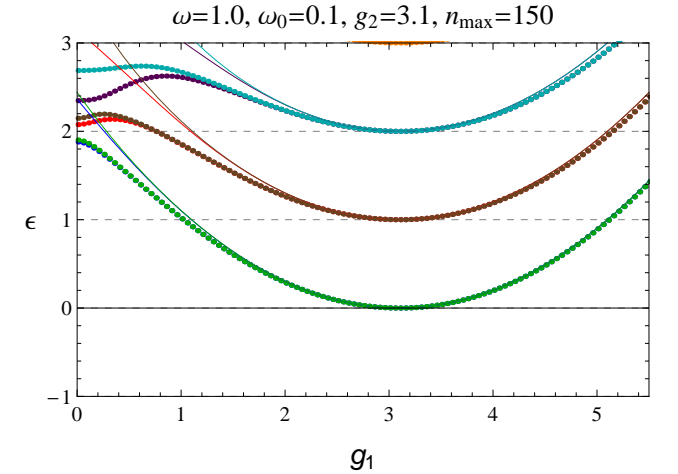


FIG. 6: Comparison of the strong-coupling quasi-degenerate harmonic ladder structure of energy spectrum as given by Eq. (96) (solid lines) and numerical diagonalization (dots) of $\hat{H}_{\text{gR}}/\omega + \frac{g_1^2 + g_2^2}{2\omega^2}$.

Hamiltonian of the generalized Rabi model (2) as

$$\hat{H}_{\text{gR}} = \hat{H}_0 - \omega \frac{g_1 g_2}{g_-^2} \hat{H}', \quad (98)$$

where $\hat{H}_0 = \omega_g \hat{A}^\dagger \hat{A} + \omega_0 \hat{\sigma}_z + g_- (\hat{A}^\dagger \hat{\sigma}_- + \hat{A} \hat{\sigma}_+) + \omega \frac{g_2^2}{g_-^2}$,

with $\omega_g \equiv \omega \frac{g_1^2 + g_2^2}{g_1 - g_2}$ and the perturbation is given by $\hat{H}' = \hat{A}^\dagger \hat{A}^\dagger + \hat{A} \hat{A}$. The Hamiltonian \hat{H}_0 has the same form as the Jaynes-Cummings Hamiltonian apart from the additional constant $\omega \frac{g_2^2}{g_-^2}$, therefore its spectrum and eigenstates are known [2]. From this it follows that the spectrum of the generalized Rabi model in the first order in \hat{H}' reads

$$E_{n,\pm}^{(0)} = \omega_g \left(n - \frac{1}{2}\right) \pm \frac{1}{2} \sqrt{(2\omega_0 + \omega_g)^2 + 4n g_-^2} + \omega \frac{g_2^2}{g_-^2}, \quad (99)$$

which is valid for small $\omega \frac{g_1 g_2}{g_-^2}$ and large ω_0 .

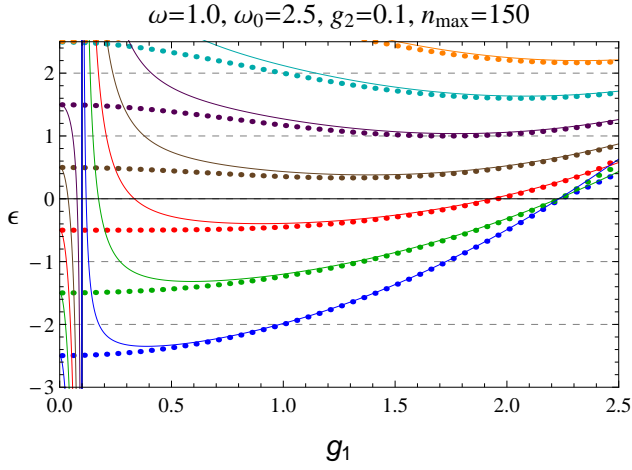


FIG. 7: Comparison of the strong-coupling and large ω_0 energy spectrum as given by Eq. (99) (solid lines) and numerical diagonalization (dots) of $\hat{H}_{\text{GR}}/\omega + \frac{g_1^2 + g_2^2}{2\omega^2}$. The perturbation theory (99) clearly fails in the region where $g_1 \approx g_2$ since then the expression $\omega \frac{g_1 g_2}{g_-^2}$ diverges. This can be seen in the plot when g_1 is equal to $g_2 = 0.1$, then the solid lines diverge and around this region the approximation (99) is not appropriate.

IV. DISCUSSION AND CONCLUSIONS

The connection between the polynomial solutions, Bethe ansatz equations and quasi-exact solvability is well known and has been discussed in the literature from different perspectives, see, e.g., [20, 25] and Refs. therein. Noticing that

$$J^+ = z^2 \frac{d}{dz} - nz, \quad J^- = \frac{d}{dz}, \quad J^0 = z \frac{d}{dz} - \frac{n}{2}, \quad (100)$$

is a differential realization of the $(n+1)$ -dimensional representation of the $sl(2)$ algebra in the Bargmann space, one can construct a bilinear combination of $J^{\pm,0}$ whose eigenstates are polynomials of the order n and smaller. This leads to a second-order differential operator which is called quasi-exactly solvable [20]. We illustrate this

construction on the simple case of $\kappa = -\nu$ of the generalized Rabi model. The differential operator acting on the function $\chi(z)$ is $(z^2 - \nu^2)d_z^2 - (2\nu(z^2 - \nu^2) + 2nz - 2\nu)d_z + 2\nu nz - \mathcal{A}$, where $-\mathcal{A} = (n - 2\lambda_+)(n + 1) - 2\nu^2$ and $d_z \equiv d/dz$. Using the operators $J^{\pm,0}$ it can be represented as $J^+ J^- - \nu^2 J^- J^- + 2\nu J^+ + 2\nu(\nu^2 + 1)J^- - nJ^0 - \mathcal{A} - n^2/2$ which has a quasi-exactly-solvable form. This predicts the existence of the exceptional part of the spectrum in the generalized Rabi model which has been studied in this paper. In particular, we found that: (i) The exceptional part of the spectrum corresponds to the level crossings; no level crossings occur outside of the exceptional points. (ii) All level crossings occur at integer values of energy $\epsilon_c = n$; the number of crossings in parameter space is always between $n + 1$ and $2n + 1$. The wave functions at these points have a polynomial structure in Bargmann space. (iii) The avoided level crossings occur at half-integer values of the energy, $\epsilon_{ac} = n/2$, at least for $g_1 \gg g_2$ (or $g_2 \gg g_1$). (iv) In the strong-coupling limit $g_1/\omega \gg 1$ and $g_2/\omega \gg 1$, the spectrum consist of the two quasi-degenerate harmonic ladders.

The obtained results for the generalized Rabi model can be used in several physical applications, namely for the two-dimensional electron gas in a magnetic field with Rashba and Dresselhaus spin-orbit couplings and for the cavity and circuit QED systems.

V. ACKNOWLEDGMENTS

This work was supported by the Swiss National Science Foundation. M.T. is grateful to IIP for hospitality.

Appendix A: Derivation of Eq. (11)

In this Appendix we show how the system of two first-order differential equations (7) and (6) can be reduced to a single second order differential equation for $\psi_1(z)$. To this end we differentiate Eq. (6) one more time and eliminate $\psi_2(z)$ from Eq. (7) and $\psi_2'(z)$ from Eq. (6). Thus, we get a second order differential equation for $\psi_1(z)$. The substitution

$$\psi_1(z) = \exp(-\nu z)\chi(z), \quad (A1)$$

yields the following differential equation for $\chi(z)$

$$A_3(z)\chi'' + B_3(z)\chi' + C_2(z)\chi = 0, \quad (A2)$$

where the polynomials are

$$A_3(z) = \sum_{j=0}^3 a_n z^j, \quad B_3(z) = \sum_{j=0}^3 b_n z^j, \quad C_2(z) = \sum_{j=0}^2 c_n z^j, \quad (A3)$$

with the corresponding coefficients given by

$$\begin{aligned} a_0 &= -\nu^2\delta, & a_1 &= \nu\lambda_-, \\ a_2 &= \delta, & a_3 &= -\frac{1}{\nu}\lambda_-, \end{aligned} \quad (\text{A4})$$

$$\begin{aligned} b_0 &= \nu(\delta - \lambda_- + 2\nu^2\delta), & b_1 &= (\delta - \lambda_- - 2\delta\epsilon - 2\nu^2\lambda_-), \\ b_2 &= \frac{2}{\nu}\epsilon\lambda_- - 2\nu\delta, & b_3 &= 2\lambda_-, \end{aligned} \quad (\text{A5})$$

$$\begin{aligned} c_0 &= -[\delta(\delta^2 - \epsilon^2 + \lambda_+) + \epsilon\lambda_-] - \nu^2(\delta - \lambda_-) - \nu^4\delta, \\ c_1 &= \frac{1}{\nu}[\delta^2\lambda_- - \delta\lambda_+ - \epsilon(e+1)\lambda_-] \\ &\quad - \nu(\delta - \lambda_- - 2\delta\epsilon) + \nu^3\lambda_-, \\ c_2 &= -2\lambda_-\epsilon. \end{aligned} \quad (\text{A6})$$

It is convenient to rewrite Eq. (A2) as

$$\left[\frac{d^2}{dz^2} + \left(\sum_{s=1}^3 \frac{\nu_s}{z - \rho_s} + \nu_0 \right) \frac{d}{dz} + \frac{D_2(z)}{\prod_{s=1}^3 (z - \rho_s)} \right] \chi(z) = 0, \quad (\text{A7})$$

where $D_2(z) = \sum_{s=0}^2 d_s z^s$ is a polynomial of degree 2 with the coefficients given by $d_j = c_j/a_3$, ρ_j are the zeros of $A_3(z)$ and we set $\frac{\delta\nu}{\lambda_-} \equiv \kappa$:

$$\begin{aligned} d_0 &= \kappa(\delta^2 - \epsilon^2 + 2\epsilon\lambda_+ - \lambda_+^2 + \lambda_+ + \nu^2 + \nu^4) \\ &\quad + \nu(\epsilon - \lambda_+ - \nu^2), \end{aligned} \quad (\text{A8})$$

$$d_1 = e(e+1) - \delta^2 + \delta\frac{\lambda_+}{\lambda_-} + \nu\kappa - \nu^2 - 2\nu\epsilon\kappa - \nu^4, \quad (\text{A9})$$

$$d_2 = 2\nu\epsilon, \quad (\text{A10})$$

$$\rho_1 = \nu, \quad \rho_2 = -\nu, \quad \rho_3 = \kappa, \quad (\text{A11})$$

$$\nu_1 = -\epsilon + 1, \quad \nu_2 = -\epsilon, \quad \nu_3 = -1, \quad \nu_0 = -2\nu. \quad (\text{A12})$$

Appendix B: Derivation of Eq. (25) and Eq. (26)

Note that we have the identities

$$\sum_{s=1}^3 \rho_s = \kappa, \quad \sum_{s=1}^3 \nu_s = -2\epsilon, \quad \sum_{s<p}^3 \rho_s \rho_p = -\nu^2, \quad (\text{B1})$$

$$\sum_{s \neq p \neq q}^3 \nu_s (\rho_p + \rho_q) = -2\epsilon\kappa - \nu + \kappa. \quad (\text{B2})$$

As already mentioned in the main text the first condition, Eq. (19), $d_2 = 2\nu\epsilon = 2\nu n$, provides us the allowed energy spectrum,

$$\epsilon = n, \quad \text{or} \quad E = \omega(n - \lambda_+). \quad (\text{B3})$$

Substituting this into the second and the third conditions, Eqs. (20), (21), gives two quadratic equations for

λ_+ and δ ,

$$2\nu Z_1 = \lambda_+^2 - \left(2n + 1 - \frac{\kappa}{\nu} \right) \lambda_+ - (\delta^2 + \nu(\nu - \kappa) + \nu^4), \quad (\text{B4})$$

$$\begin{aligned} 2\nu^2 Z_2 &= -\lambda_+^2 + (2n + 1 - \frac{\kappa}{\nu} + \kappa^2 - \nu^2) \lambda_+ \\ &\quad + (\delta^2 + \nu(\nu - \kappa) + \kappa^2 \nu^2 + 2n\nu^2(\nu^2 + 1)). \end{aligned} \quad (\text{B5})$$

Using the identity $\lambda_+^2 - \lambda_-^2 = \nu^4$ and that $\lambda_- = \delta\nu/\kappa$ we can express λ_+ in terms of δ as $\lambda_+ = \sqrt{\delta^2 \frac{\nu^2}{\kappa^2} + \nu^4}$.

Appendix C: Procedure for solving the Bethe ansatz equations (23)

In this appendix we present in detail the procedure for determining the values of the parameters ω , ω_0 , g_1 , g_2 at which the eigenfunctions $\chi(z)$ are polynomials of finite order. At those points the energy levels cross and the eigenstates are doubly degenerated. As described in the main text to determine those parameters we have to solve the Bethe ansatz equations (23) regarding the conditions given by Eqs. (25), (26) and $\epsilon = n$.

Let us consider the Bethe ansatz equations

$$\sum_{j \neq i}^n \frac{2}{z_j - z_i} + \frac{\epsilon - 1}{z_i - \nu} + \frac{\epsilon}{z_i + \nu} + \frac{1}{z_i - \kappa} + 2\nu = 0, \quad (\text{C1})$$

with $i = 1, 2, \dots, n$ and where we have to fix $\epsilon = n$.

These equations essentially correspond to the Bethe ansatz equations which allow (through their solutions) to define the eigenstates of a Reduced BCS (or Richardson) Hamiltonian [37, 38]. In fact, by introducing the notation $\epsilon_1 = \nu$, $\epsilon_2 = -\nu$, $\epsilon_3 = \kappa$ and $d_1 = n - 1$, $d_2 = n$, $d_3 = 1$ we can write the corresponding Richardson equations in the form

$$r_i := \sum_{j \neq i}^n \frac{2}{z_j - z_i} + \sum_{j=1}^3 \frac{d_j}{z_i - \epsilon_j} + 2\nu = 0. \quad (\text{C2})$$

Furthermore, it has been shown [27] that introducing the change of variables

$$\Lambda_j = \frac{1}{2\nu} \sum_{k=1}^n \frac{1}{\epsilon_j - z_k} \quad (\text{C3})$$

the quadratic equation

$$(1 - d_j)\Lambda_j^{(1)} + \Lambda_j^2 - \Lambda_j - \frac{1}{2\nu} \sum_{i \neq j}^3 d_i \frac{\Lambda_i - \Lambda_j}{\epsilon_i - \epsilon_j} = 0 \quad (\text{C4})$$

together with its derivatives

$$\begin{aligned} \mathcal{E}_j^{(l)} := & \left(1 - \frac{d_j}{l+1}\right) \Lambda_j^{(l+1)} + \sum_{k=0}^l \binom{l}{k} \Lambda_j^{(k)} \Lambda_j^{(l-k)} \\ & - \Lambda_j^{(l)} - l! \sum_{i \neq j}^3 d_i \left(\frac{1}{(2\nu)^{l+1}} \frac{\Lambda_i - \Lambda_j}{(\epsilon_i - \epsilon_j)^{l+1}} \right. \\ & \left. - \sum_{m=1}^l \frac{1}{(2\nu)^m} \frac{\Lambda_j^{(l-m+1)}}{(l-m+1)!} \frac{1}{(\epsilon_i - \epsilon_j)^m} \right) = 0 \end{aligned} \quad (\text{C5})$$

for $j = 1, 2, 3$ and $l = 1, \dots, d_j - 1$ form a closed system of equations which is satisfied whenever the rapidities z_k satisfy the Richardson equations (C2).

Consider now Eq. (C2), by using the following relations

$$\begin{aligned} \sum_{i=1}^n \sum_{j \neq i}^n \frac{1}{z_i - z_j} &= 0, \\ \sum_{i=1}^n \sum_{j \neq i}^n \frac{z_i}{z_i - z_j} &= \frac{n(n-1)}{2}, \\ \sum_{i=1}^n \sum_{j \neq i}^n \frac{z_i^2}{z_i - z_j} &= (n-1) \sum_{i=1}^n z_i \end{aligned} \quad (\text{C6})$$

and by taking the sums $\sum_{i=1}^n r_i$, $\sum_{i=1}^n r_i z_i$, $\sum_{i=1}^n z_i^2 r_i$ we obtain

$$\begin{aligned} n - \sum_{l=1}^3 d_l \Lambda_l &= 0, \\ -n(n-1) + n \sum_{l=1}^3 d_l - 2\nu \sum_{l=1}^3 d_l \epsilon_l \Lambda_l + 2\nu Z_1 &= 0, \\ -2(n-1)Z_1 + \sum_{l=1}^3 d_l Z_1 + n \sum_{l=1}^3 d_l \epsilon_l - 2\nu \sum_{l=1}^3 d_l \epsilon_l^2 \Lambda_l \\ + 2\nu Z_2 &= 0. \end{aligned} \quad (\text{C7})$$

To derive these equations we used the change of variables introduced in Eq. (C3). Eq. (C7) is linear in the variables $\Lambda_{1,2,3}$ and can be readily solved, we find

$$\begin{aligned} \Lambda_1 &= \frac{-n^2(\kappa + \nu) + 2\nu n(\kappa\nu - 1) - 2Z_1(\kappa\nu + \nu^2 - 1) + 2\nu Z_2}{4\nu^2(\kappa + \nu)}, \\ \Lambda_2 &= \frac{n^2(\nu - \kappa) - 2\kappa\nu^2 n + Z_1(-2\kappa\nu + 2\nu^2 + 2) + 2\nu Z_2}{4\nu^2(n-1)(\nu - \kappa)}, \\ \Lambda_3 &= \frac{\kappa n - 2\nu^3 n - \nu n + 2Z_1 + 2\nu Z_2}{2\kappa^2\nu - 2\nu^3}. \end{aligned} \quad (\text{C8})$$

Finally by solving Eq. (C4), with $j = 1$, for $\Lambda_1^{(1)}$ and each successive derivative (Eq. (C5)) for $\Lambda_1^{(l)}$ (with $l = 1, \dots, d_1 - 1$) and then replacing Z_1 and Z_2 by the expressions given in Eq. (25) and Eq. (26), we get at last a polynomial equation as a function of the parameters κ, ν

and δ (since the first term containing the next derivative will cancel due to the prefactor $1 - d_1/(d_1 - 1 + 1) = 0$). Let us denote this equation by $p_n(\kappa, \nu, \delta)$. The zeros of this polynomial equation, $p_n(\kappa, \nu, \delta) = 0$, will at the end determine the position of the energy level crossings. This procedure can be used to determine the positions of the crossings for all $n > 1$, for the specific case $n = 1$, the Bethe ansatz equations (C1) can be easily solved

$$z_1^{(\pm)} = \frac{\kappa\nu - \nu^2 - 1 \pm \sqrt{\nu^2(\kappa + \nu)^2 + 1}}{2\nu}. \quad (\text{C9})$$

It is clear that because of the particular form of ν and κ as functions of g_1 and g_2

$$\nu = \frac{\sqrt{g_1 g_2}}{\omega}, \quad \kappa = \frac{2\delta\omega\sqrt{g_1 g_2}}{g_1^2 - g_2^2}, \quad \delta = \frac{\omega_0}{\omega}, \quad (\text{C10})$$

a singularity will appear whenever we will be in the region $g_1 \sim g_2$. Therefore, the particular case $g_1 = g_2 = g$ has to be treated separately.

1. Rabi limit: $g_1 = g_2 = g$

In this case the corresponding Schrödinger equation reads

$$A_2(z)\chi''(z) + B_2(z)\chi'(z) + C_1(z)\chi(z) = 0, \quad (\text{C11})$$

where

$$A_2(z) = \delta(z - \nu)(z + \nu), \quad (\text{C12})$$

$$B_2(z) = \delta\nu(1 + 2\nu^2) + \delta(1 - 2\epsilon)z - 2\nu\delta z^2, \quad (\text{C13})$$

$$C_1(z) = -\delta(\nu^4 + \nu^2 + \delta^2 - \epsilon^2 + \lambda_+) - \left(\frac{\delta}{\nu}\lambda_+\right)z. \quad (\text{C14})$$

By noticing that for $g_1 = g_2 = g$ we have $\lambda_+ = \nu^2$ and dividing the Schrödinger equation (C11) by $A_2(z)$ we get

$$\left[\frac{d^2}{dz^2} + \left(\frac{1 - \epsilon}{z - \nu} + \frac{-\epsilon}{z + \nu} - 2\nu \right) \frac{d}{dz} - \frac{2\nu^2(1 + \epsilon) + \delta^2 - \epsilon^2 + 2\nu(1 - \epsilon)z}{(z - \nu)(z + \nu)} \right] \chi(z) = 0. \quad (\text{C15})$$

According to the Eqs. (A.12)-(A.15) in [25] this differential equation has a polynomial solution $\chi(z) = \prod_{i=1}^n (z - z_i)$ of degree n if

$$-2\nu(1 - \epsilon) = -n(-2\nu), \quad (\text{C16})$$

$$-(2\nu^2(1 + \epsilon) + \delta^2 - \epsilon^2) = 2\nu Z_1 - n(n-1) - n(1 - 2\epsilon), \quad (\text{C17})$$

where $Z_1 = \sum_{i=1}^n z_i$ and z_i are given by the roots of the following, now much simpler, Bethe ansatz equations

$$\sum_{j \neq i}^n \frac{2}{z_j - z_i} + \frac{\epsilon - 1}{z_i - \nu} + \frac{\epsilon}{z + \nu} + 2\nu = 0. \quad (\text{C18})$$

A similar procedure to determine the values of the parameters for which the eigenfunctions $\chi(z)$ are polynomial, and where the energy levels cross, can once again be applied. With the only difference that, because of the missing term in Eq. (C18)

$$\frac{1}{z_i - \kappa} \rightarrow 0, \quad (\text{C19})$$

we will get a linear system of only two equations. This is consistent since the condition for Z_2 does not apply anymore in this case. In view of Eq. (C16) and Eq. (C17), we now have to satisfy the condition

$$2\nu Z_1 = -2\nu^2(n+2) - \delta^2 + 1 \quad (\text{C20})$$

and we have to fix $\epsilon = n+1$ in Eq. (C18). Thus we obtain

$$\Lambda_1 = \frac{2\nu Z_1 + n(n+2+2\nu^2)}{4\nu^2 n},$$

$$\Lambda_2 = -\frac{2\nu Z_1 + n(n+2-2\nu^2)}{4\nu^2(n+1)}. \quad (\text{C21})$$

In Fig. 8 we show the crossings of the energy levels in the Rabi limit, $g_1 = g_2 = g$. The energy spectrum was calculated numerically, by truncating the bosonic Hilbert space at $n_{\max} = 200$. The level crossings were obtained

using the method explained above and are indicated by the black markers.

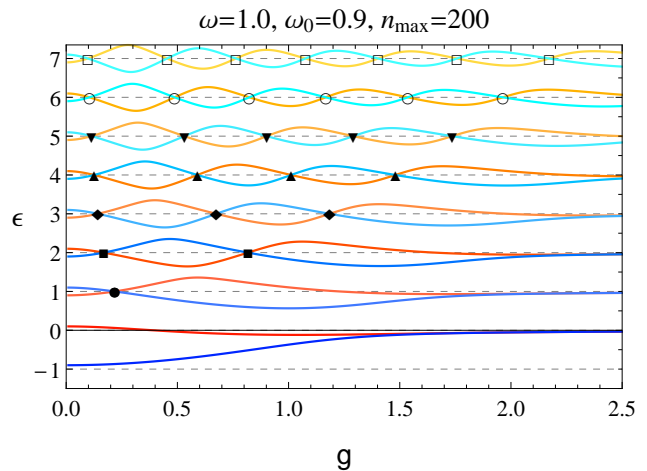


FIG. 8: Plot of the energy spectrum of the Rabi model ($g_1 = g_2 = g$) obtained by numerical diagonalization. The energy level crossings are indicated by the black markers, which were calculated using the method outlined in this Appendix.

-
- [1] I. I. Rabi, Phys. Rev. **49**, 324 (1936); **51**, 652 (1937).
[2] E. T. Jaynes and F. W. Cummings, Proc. Inst. Elect. Eng. **51**, 89 (1963); F. W. Cummings, Phys. Rev. **140**, A1051 (1965).
[3] D. Braak, Phys. Rev. Lett. **107**, 100401 (2011).
[4] A. Moroz, arXiv:1205.3139 (2012); Europhys. Lett. **100**, 60010 (2012); Ann. Phys. (N.Y.) **338**, 319-340 (2013).
[5] F. Beaudoin, J. M. Gambetta, and A. Blais, Phys. Rev. A **84**, 043832 (2011).
[6] S. Haroche and J. M. Raimond, *Exploring the Quantum: Atoms, Cavities and photons*, (Oxford, Oxford University Press, 2006).
[7] D. I. Schuster *et al.*, Nature **445** 515 (2007); M. Hofheinz *et al.*, Nature **459** 546 (2009).
[8] P. Forn-Diaz *et al.*, Phys. Rev. Lett. **105** 237001 (2010); T. Niemczyk *et al.*, Nature Phys. **6**, 772 (2010).
[9] I. D. Feranchuk, L. I. Komarov, and A. P. Ulyanenkov, J. Phys. A: Math. Gen. **29**, 4035 (1996).
[10] J. Hausinger and M. Grifoni, New J. Phys. **10**, 115015 (2008).
[11] E. K. Irish, J. Gea-Banacloche, I. Martin, and K. C. Schwab, Phys. Rev. B **72**, 195410 (2005).
[12] J. Casanova, G. Romero, I. Lizuain, J. J. Garcia-Ripoll, and E. Solano, Phys. Rev. Lett. **105**, 263603 (2010).
[13] B. R. Judd, J. Phys. C **12**, 1685 (1979).
[14] H. G. Reik, H. Nusser, and L. A. Amarante Ribeiro, J. Phys. A **15**, 3491 (1982).
[15] M. Kuś, J. Math. Phys. **26**, 2792 (1985).
[16] M. Kuś and M. Lewenstein, J. Phys. A: Math. Gen. **19**, 305 (1986).
[17] H. G. Reik and M. Doucha, Phys. Rev. Lett. **57**, 787 (1986).
[18] R. Koc, M. Koca, and H. Tütüncüler, J. Phys. A: Math. Gen. **35**, 9425 (2002).
[19] C. Emary and R. F. Bishop, J. Math. Phys. **43**, 3916 (2002).
[20] A. V. Turbiner, arXiv:hep-th/9409068.
[21] M. Jeleńska-Kuklińska and M. Kuś, Phys. Rev. A **41**, 2889 (1990).
[22] S. I. Erlingsson, J. C. Egues, and D. Loss, Phys. Rev. B **82**, 155456 (2010).
[23] M. Schiró, M. Bordyuh, B. Öztöp, and H. E. Türeci, Phys. Rev. Lett. **109**, 053601 (2012).
[24] A. L. Grimsmo and S. Parkins, Phys. Rev. A **87**, 033814 (2013).
[25] Y.-Z. Zhang, J. Phys. A: Math Theor. **45**, 065206 (2012).
[26] E. K. Sklyanin, Zap. nauch. semin. LOMI **134**, 112 (1983).
[27] A. Faribault, O. El Araby, C. Sträter, and V. Gritsev, Phys. Rev. B **83**, 235124 (2011); O. El Araby, V. Gritsev, and A. Faribault, Phys. Rev. B **85**, 115130 (2012).
[28] I. Marquette and J. Links, J. Stat. Mech. (2012) P08019; F. Pan *et al.*, J. Phys. A: Math. Theor. **44**, 395305 (2011).
[29] J. Dukelsky, S. Pittel, and G. Sierra, Rev. Mod. Phys. **76**, 643 (2004).
[30] M. E. H. Ismail, Pacific J. Math. **193**, 335 (2000); M. E. H. Ismail in *Random Matrix models and Their Applications*

tions, (Cambridge University Press, 2001).

- [31] D. Mattis and E. Lieb, J. Math. Phys. **2**, 602 (1961).
 [32] M. Brune, S. Haroche, J. M. Raimond, L. Davidovich, and N. Zagury, Phys. Rev. A **45**, 5193 (1992).
 [33] S. De Baerdemacker, Phys. Rev. C **86**, 044332 (2012).
 [34] E. A. Yuzbashyan, A. A. Baytin, and B. L. Altshuler, Phys. Rev. B **68**, 214509 (2003).
 [35] A. B. Klimov and S. M. Chumakov, *A Group-Theoretical*

Approach to Quantum Optics, (Wiley-VCH, 2009).

- [36] V. V. Albert, G. D. Scholes, and P. Brumer, Phys. Rev. A **84**, 042110 (2011).
 [37] R. Richardson, Phys. Lett. **3**, 277 (1963).
 [38] R. Richardson and N. Sherman, Nucl. Phys. **52**, 221 (1964).

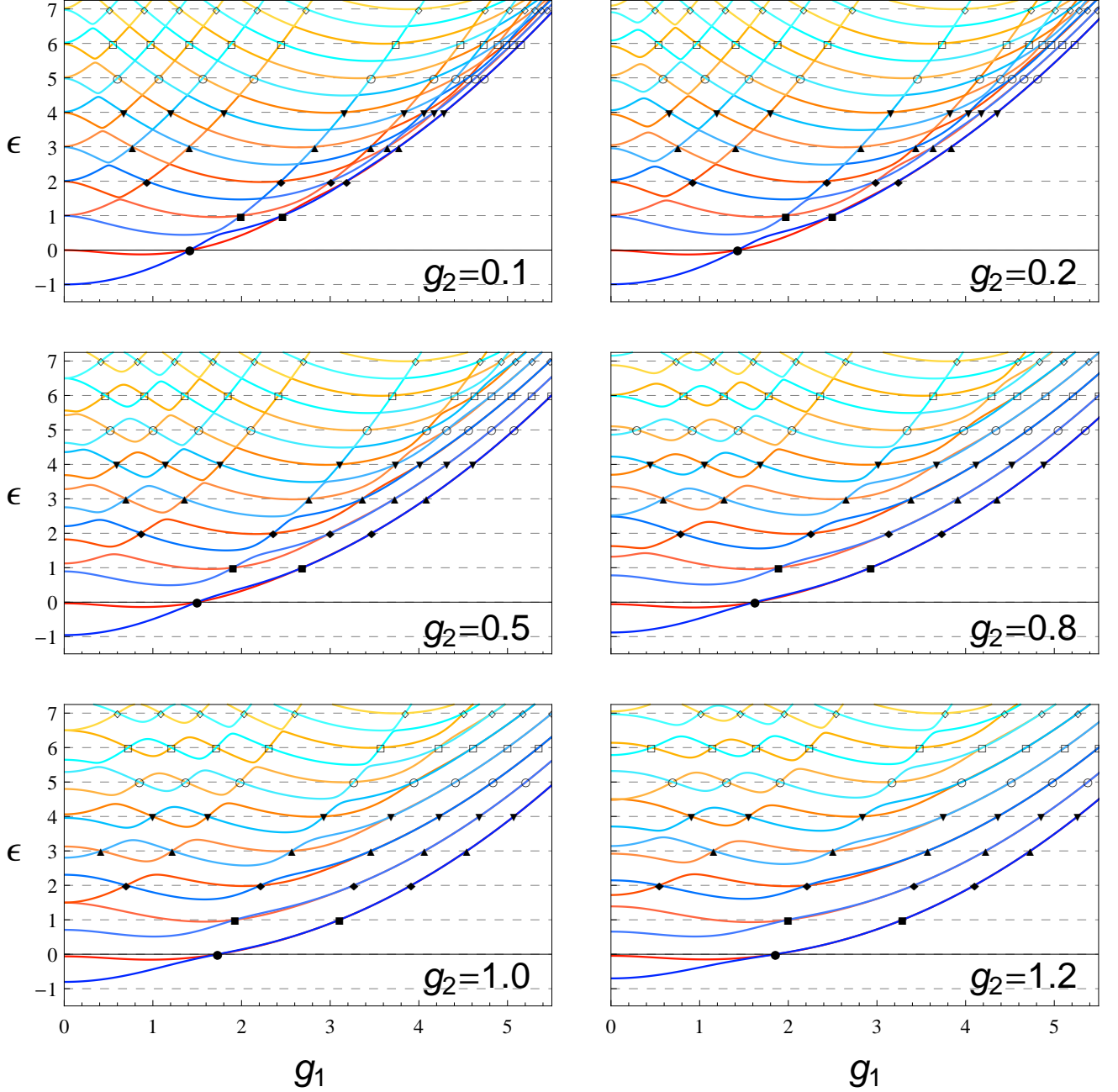


FIG. 9: Energy spectrum of the generalized Rabi model shifted by $(g_1^2 + g_2^2)/(2\omega^2)$ as a function of the coupling g_1 for a range of couplings g_2 . Black markers at integer energies $\epsilon = n$ indicate the energy levels intersection points, where the model has an exceptional spectrum. No other level crossings occur at different points. The level repulsion happens at the half-integer values of energy.